

Editing and escape from editing in anti-DNA B cells

Salar N. Khan*, Esther J. Witsch†, Noah G. Goodman‡, Anil K. Panigrahi‡, Ching Chen§, Yufei Jiang¶, Amy M. Cline*, Jan Erikson||, Martin Weigert†***, Eline T. Luning Prak‡, and Marko Radic*††

*Department of Molecular Sciences, University of Tennessee Health Science Center, Memphis, TN 38163; †Department of Pathology and The Gwen Knapp Center for Lupus and Immunology Research, University of Chicago, Chicago, IL 60637; ‡Department of Pathology and Laboratory Medicine, University of Pennsylvania School of Medicine, Philadelphia, PA 19104; §Department of Pathology, University of Maryland School of Medicine, Baltimore, MD 21201; ¶Vaccine Branch, National Naval Medical Research Center, National Cancer Institute/National Institutes of Health, Baltimore, MD 20889; and ||Program of Immunology, The Wistar Institute, Philadelphia, PA 19104

Contributed by Martin Weigert, January 11, 2008 (sent for review October 8, 2007)

Tolerance to dsDNA is achieved through editing of Ig receptors that react with dsDNA. Nevertheless, some B cells with anti-dsDNA receptors escape editing and migrate to the spleen. Certain anti-dsDNA B cells that are recovered as hybridomas from the spleens of anti-dsDNA H chain transgenic mice also bind an additional, Golgi-associated antigen. B cells that bind this antigen accumulate intracellular IgM. The intracellular accumulation of IgM is incomplete, because IgM clusters are observed at the cell surface. In the spleen, B cells that express the heavy and light chains encoding this IgM are surface IgM-bright and acquire the CD21-high/CD23-low phenotype of marginal zone B cells. Our data imply that expression of an Ig that binds dsDNA and an additional antigen expressed in the secretory compartment renders B cells resistant to central tolerance. In the periphery, these B cells may be sequestered in the splenic marginal zone.

autoantibodies | B cell development | receptor editing

Receptor editing replaces autoreactive B cell receptors (BCR) with nonautoreactive BCR (1, 2). It is accomplished through secondary rearrangement of upstream Ig light (L) (3–5) or heavy (H) chain (6) variable (V) genes. Autoreactive B cells that would otherwise be deleted (7, 8) use editing to revise their receptors and exit from the bone marrow. Given the high frequency of autoreactivity among immature B cells (9), receptor editing plays a major role in determining the size and shape of the mature B cell repertoire (10, 11).

This mechanism also yields incompletely or partially edited B cells. Incompletely edited BCR retain some self-reactivity and/or gain new auto-specificities. B cells expressing such BCR are a liability because they are activated in lupus-susceptible mice and during induction of lupus (12–15). They can evolve to pathogenic effector cells by mutation and class switch. This pathway to autoimmunity is illustrated by 3H9, a typical pathogenic anti-DNA expressed by a diseased mouse (16). By reverting the somatically mutated VH3H9 to its germ-line sequence, it was discovered that the precursor of 3H9 bound to phosphatidylserine (PS) (17). Subsequent mutations gave rise to 3H9, an Ab with reactivity toward dsDNA, nucleosomes, and additional phospholipids (18–21). Thus, an incompletely edited B cell may have been the precursor of this pathogenic autoantibody.

Partial editing leads to coexpression of L chains, one of which is autoreactive. The autoreactive H/L combination escapes central tolerance and gains access to the periphery because, we presume, the nonautoreactive H/L pair dilutes the expression of the autoreactive pair. Since we discovered this type of partially edited B cell, many examples of allelic or isotypic inclusion have been observed (15, 22–25), including additional transgenic (Tg)-encoded autoreactivities (26, 27) and autoreactivities present within an unperturbed repertoire (11, 28). Such B cells have been referred to as “Trojan horses” and may, if activated in the periphery, pose a risk of autoimmunity.

Here we describe an incompletely edited anti-dsDNA B cell that is regulated in a novel way: This B cell retains anti-dsDNA reactivity and acquires specificity for a Golgi-associated anti-

gen. Its antibodies accumulate in the cell interior, bound to the Golgi apparatus. The most direct interpretation of our results argues that the altered site of BCR expression allows these B cells to escape central tolerance and accumulate in the periphery. This mechanism may conceal a partially edited or unedited autoantibody-expressing B cell.

Results

We have recreated the splenic B cell repertoires of three H chain Tg mice (Fig. 1) *in vitro* and observed that VH/VL pairs expressed in the spleen do not bind to dsDNA. However, we also discovered an exception: VH/VL pairs incorporating the editor V κ 38c retained affinity for dsDNA yet were expressed in the spleen. To explore why central tolerance is unable to regulate these anti-dsDNA VH/VL pairs, we examined their cellular distribution in hybridomas and their expression in splenic B cell subsets.

Analysis of Autoreactivity. The repertoire in anti-dsDNA H chain Tg mice is highly biased toward editor L chains (Fig. 1). The IgM antibodies encoded by the Tg H and editor L chains bind DNA poorly or not at all (22). However, to evaluate the role of receptor editing in anti-dsDNA binding, one must compare the expressed H/L pairs to the “missing” H/L pairs, i.e., to those H/L pairs that are the precursors of receptor editing and thus are excluded from the peripheral repertoire. To analyze the missing VH/VL pairs, we re-derived and expressed them as bivalent single-chain Fv (scFv) in *Escherichia coli*. For comparison, we generated VH/VL pairs that are expressed in anti-DNA H chain Tg mice. The structure of the recombinant VH/VL pairs provided a technical advantage over the IgM antibodies: The bivalent binding of our scFv made them useful substitutes for measuring BCR interactions with antigen. All together, we constructed nine scFv, five to represent VH/VL pairs expressed in the spleen and four to represent pairs that are missing from the peripheral repertoire (see [supporting information \(SI\) Text and SI Fig. 6](#)).

Our initial analysis focused on the most closely related VH/VL pairs: those in which a single residue in VH determines whether a VL participates in the splenic B cell repertoire or not (Fig. 1). Thus, we compared VH3H9+V κ 12/13, a pair that accounts for 64% of the repertoire in VH3H9 mice (Fig. 1A), to

Author contributions: S.N.K., E.J.W., E.T.L.P., and M.R. designed research; S.N.K., E.J.W., N.G.G., A.K.P., Y.J., and A.M.C. performed research; C.C. and J.E. contributed new reagents/analytic tools; S.N.K., E.J.W., N.G.G., A.K.P., C.C., Y.J., A.M.C., J.E., M.W., E.T.L.P., and M.R. analyzed data; and S.N.K., E.J.W., M.W., E.T.L.P., and M.R. wrote the paper.

The authors declare no conflict of interest.

**To whom correspondence may be addressed. E-mail: mweigert@bsd.uchicago.edu.

††To whom correspondence may be addressed at: Department of Molecular Sciences, University of Tennessee Health Science Center, 858 Madison Avenue, Memphis, TN 38163. E-mail: mradic@utm.edu.

This article contains supporting information online at www.pnas.org/cgi/content/full/0800025105/DC1.

© 2008 by The National Academy of Sciences of the USA

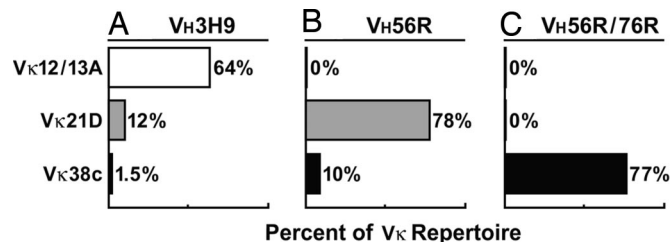


Fig. 1. H chain Tg BALB/c mice show drastic differences in their L chain repertoires. The endogenous L chain repertoires in anti-DNA H chain Tg mice have previously been analyzed by constructing LPS hybridomas from splenic B cells (4, 22). V κ 12/13A predominates in hybridomas from VH3H9 mice, with V κ 21D and V κ 38c following at lower percentages (A). V κ 12/13A is absent in VH56R Tg mice (22), whereas V κ 21D predominates and V κ 38c is less prevalent (B). V κ 38c is abundant in VH56R/76R Tg mice (22), whereas V κ 12/13A and V κ 21D are absent (C). Additional V κ are expressed at low frequencies but are not represented in the figure.

VH56R+V κ 12/13, a pair that is absent from the repertoire in VH56R mice (Fig. 1B). We also compared VH56R+V κ 21D, a pair that accounts for 78% of the repertoire in VH56R mice (Fig. 1B), to VH56R/76R+V κ 21D, a pair that is absent from the repertoire of VH56R/76R mice (Fig. 1C). The absence of V κ 12/13 from the VH56R repertoire results from the single replacement of Asp in VH3H9 by Arg at position 56 in VH56R. Similarly, the absence of V κ 21D from the VH56R/76R repertoire is a result of introducing a second Arg (at position 76) into the VH56R/76R Tg. Because these Args increase the affinity of the VH for dsDNA (18), we predicted that the missing pairs would provide an insight into how increased dsDNA binding limits the number of acceptable editor L chains.

Indeed, these scFvs displayed a gradient of binding to dsDNA with VH/VL pairs that are expressed in the spleen having little or no dsDNA binding and pairs that are absent from the repertoire

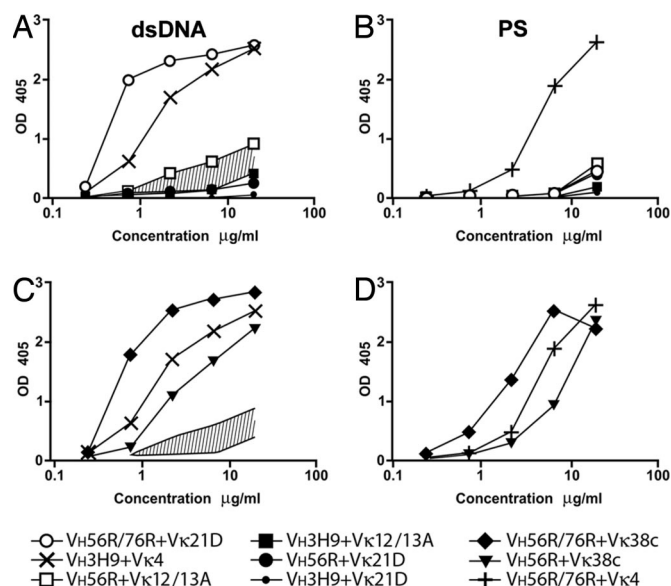


Fig. 2. Binding of bivalent scFv to dsDNA and PS in ELISA. At the given concentrations of scFv, absorbance was measured at 405 nm. VH3H9+V κ 4 and VH56R/76R+V κ 4 were used as positive controls for dsDNA (A and C) and PS (B and D) binding, respectively. The area shaded in A and C indicates a range of relative anti-DNA affinities that includes a proposed threshold of DNA binding responsible for inducing receptor editing. The H/L pairs that are represented in the repertoire fall below the threshold, and those that are absent bind DNA above the threshold. H/L pairs that incorporate V κ 38c exceeded the proposed threshold and react strongly with dsDNA (C) and PS (D).

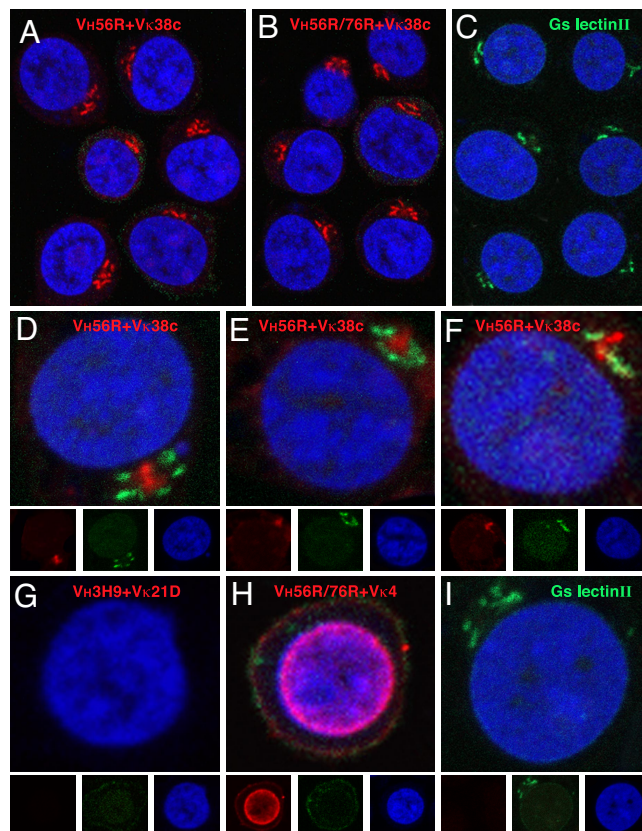


Fig. 3. Analysis of scFv binding to Jurkat cells. scFv binding to fixed and permeabilized cells was visualized with Alexa Fluor 647 rabbit anti-mouse IgG (displayed in red) and nuclei with Sytox Orange (blue). The VH56R+V κ 38c (A) and VH56R/76R+V κ 38c (B) scFv bind to a perinuclear domain composed of tubular bundles and lamellar stacks that likely corresponds to the Golgi apparatus. Binding of Alexa Fluor 488 lectin II (green) identifies terminal GlcNAc moieties that are enriched in the Golgi (C). The VH56R+V κ 38c scFv is surrounded by lectin II-reactive domains (D–F). VH3H9+V κ 21D scFv does not bind to Jurkat cells (G), whereas VH56R/76R+V κ 4 scFv binds predominantly to the nucleus (H). (I) Image of lectin II binding. Separate RGB channels are shown at one-third size below the composite color images for D–I. Binding of scFv to Jurkat cells was indistinguishable from the binding to mouse thymocytes.

exhibiting avid binding (Fig. 2A). Hence, the binding curves of VH3H9+V κ 12/13 and VH56R+V κ 12/13 define the upper and lower boundaries of the interval of relative anti-dsDNA affinities that contains the threshold between affinities that allow B cell maturation and affinities that prevent it (Fig. 2A).

DNA and PS Binding of V κ 38c Combinations. The V κ 38c contributes to the B cell repertoire in VH56R mice (Fig. 1B), and it is the predominant V κ in VH56R/76R mice (Fig. 1C). Therefore, we expected that V κ 38c would have characteristics of L chains that edit anti-dsDNA specificity, i.e., reduced avidity for dsDNA. In previous experiments with hybridoma-derived IgM (15, 22), the effect of V κ 38c on dsDNA binding was unclear because hybridomas often coexpressed V λ 1, a L chain that is an effective dsDNA binder (18).

The present experiments established that pairs between V κ 38c and either VH56R or VH56R/76R do indeed bind DNA (Fig. 2C). In addition, both VH/VL pairs bound avidly to PS (Fig. 2D). We compared the V κ 38c VH/VL pairs to the VH3H9+V κ 4 pair used by the 3H9 autoantibody, an anti-dsDNA that is excluded from the peripheral repertoire (8). The VH56R+V κ 38c pair bound dsDNA nearly as well as VH3H9+V κ 4, whereas VH56R/76R+V κ 38c bound four times better (Fig. 2C). To account for

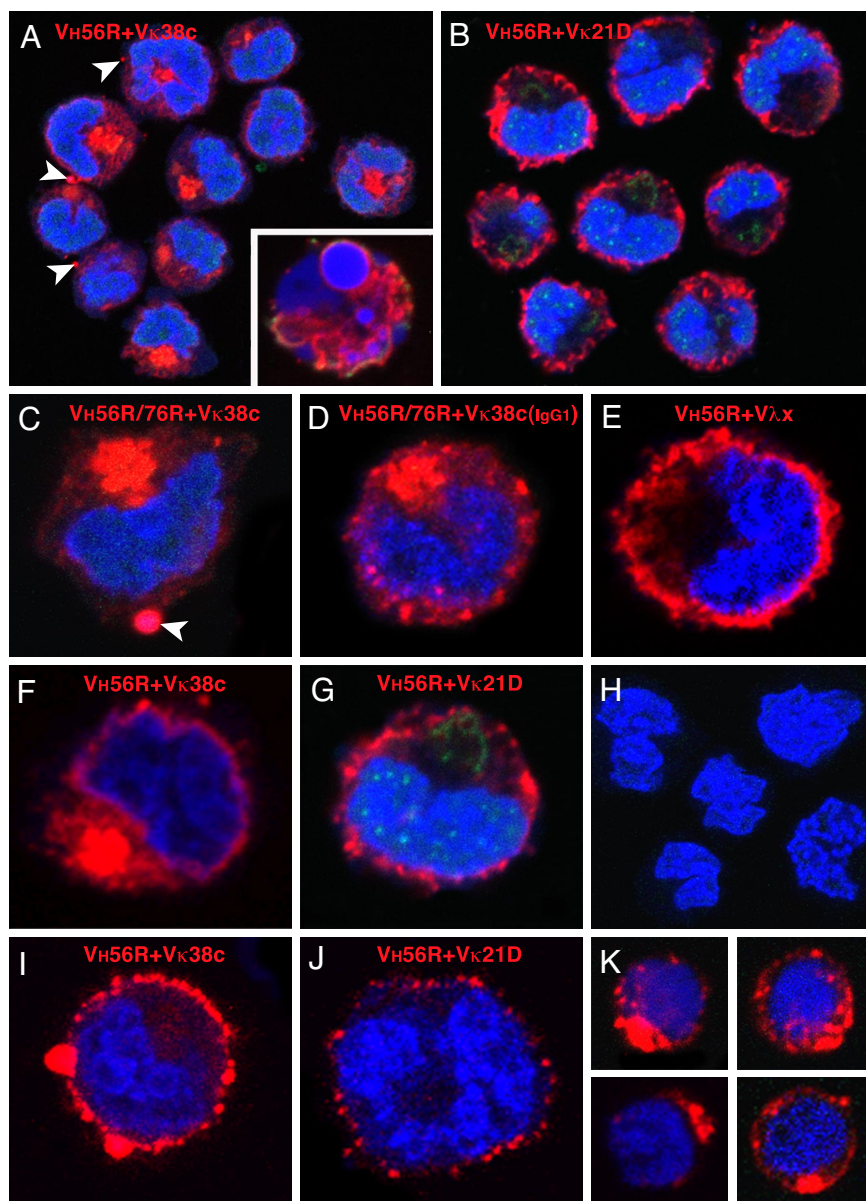


Fig. 4. Distribution of IgM in B cell hybridomas and primary B cells. VH56R+V κ 38c (A) and VH56R+V κ 21D (B) hybridoma cells were fixed, permeabilized, and incubated with Alexa Fluor 647 goat anti-mouse IgM (red), Alexa Fluor 488 lectin II (green), and Sytox Orange (blue). The VH56R+V κ 38c IgM accumulate inside the cell (A). Cultures of VH56R+V κ 38c contain cells with fragmented nuclei and apoptotic phenotype (*Inset*). In contrast, VH56R+V κ 21D IgM are localized on or close to the cell surface, and little or no Ig is retained inside the cell (B). (C and F) Individual cells producing VH56R/76R+V κ 38c (C) or VH56R+V κ 38c (F) IgM. Arrowheads in A and C indicate IgM clusters at the cell surface. (D) Hybridoma expressing VH56R/76R+V κ 38c IgG1 shows a similar intracellular accumulation of the Ig but smaller clusters at the plasma membrane. Individual VH56R+V λ x (E) and VH56R+V κ 21D (G) hybridoma cells show IgM receptors that are distributed at or near the cell surface. Cells that have lost expression of IgM do not bind to the goat anti-mouse Abs (H). VH56R+V κ 38c hybridomas that were incubated with anti-mouse IgM, then fixed and stained with Sytox orange, show cell surface clusters of IgM (I). VH56R+V κ 21D hybridomas, when treated the same, show reduced levels of surface IgM (J). B cells from the spleen of a VH56R mouse that were sorted for low surface IgM^a, then grown in culture for 48 h, fixed, and stained as in A, show cytoplasmic IgM aggregates (K). Discrete clusters of IgM appear at the cell surface. Thus, the IgM distribution in 35% of primary B cells is strikingly similar to the IgM distribution in VH56R+V κ 38c hybridomas.

the presence of avid anti-dsDNA receptors in the splenic B cell repertoire, we considered that additional autospecificities could affect expression of these BCR. Consistent with this idea, previous work on anti-dsDNA autoantibodies found that they often react with other autoantigens, such as chromatin, ribonucleoproteins, or membrane lipids (29).

Specificity of VH/VL Pairs for Intracellular Antigens. To test whether the anti-dsDNA VH/VL have an additional autospecificity, we used Jurkat T cells as a source of diverse antigens. Indeed,

immunohistochemistry revealed that the VH56R+V κ 38c and VH56R/76R+V κ 38c scFv bound to an area adjacent to the nucleus (Fig. 3A and B), whereas VH3H9+V κ 21D did not show intracellular binding (Fig. 3G), and VH56R/76R+V κ 4 bound preferentially to nuclear antigens (Fig. 3H).

The location of the VH56R+V κ 38c and VH56R/76R+V κ 38c binding and its distribution in the form of lamellar stacks and tubular bundles suggested binding to stacks and projections of the Golgi. The scFv binding paralleled the binding of *Griffonia simplicifolia* lectin II, a lectin that binds terminal GlcNAc sugars

enriched in the Golgi (Fig. 3C). To account for the binding of VH56R+V κ 38c and VH56R/76R+V κ 38c scFv to the Golgi, we considered whether the scFv and the lectin bind to terminal GlcNAc moieties. However, we observed only limited colocalization between the VH56R+V κ 38c scFv and lectin II despite the fact that both bound in the immediate vicinity of each other (Fig. 3D–F). Because the binding of the scFv was more limited and diffuse in the presence of the lectin (Fig. 3D–F) than in its absence (Fig. 3A), it is likely that the lectin sterically hinders access of the scFv to its antigen. Although the identity of the intracellular antigen bound by the VH56R+V κ 38c scFv is not known, Abs to golgin-95 provide a reliable marker for its location (S.N.K. and M.R., unpublished observations).

Distribution of Ig in Hybridomas. The binding of VH56R+V κ 38c and VH56R/76R+V κ 38c IgM to a Golgi antigen may alter the intracellular distribution of IgM *in situ*. To assess this possibility, we examined hybridomas expressing V κ 38c from VH56R and VH56R/76R Tg C57BL/6 mice (14, 15). Both VH56R+V κ 38c (Fig. 4A and F) and VH56R/76R+V κ 38c (Fig. 4C and D) IgM formed a dense aggregate in the interior of the hybridoma cells. In contrast, the IgMs with other editors, VH56R/V κ 21D (Fig. 4B and G) or VH56R/V λ x (Fig. 4E), were distributed at or just beneath the cell surface, leaving the center of the cell free of Ab. Therefore, the specificity of the Tg VH and V κ 38c pairs leads to the accumulation of IgM in the interior of the cells and may reflect binding between the newly synthesized IgM and an antigen that is expressed in the Golgi.

Because IgM and IgG isotypes differ in their assembly requirements, we tested whether constant region isotype affects intracellular retention. We took advantage of the fact that B cells expressing VH56R/76R+V κ 38c switch to IgG in MRL-lpr/lpr mice (30). IgG hybridomas derived from autoimmune VH56R/76R mice express predominantly V κ 38c (30). Analysis of VH56R/76R+V κ 38c IgG hybridomas demonstrated that class switch did not change the intracellular accumulation of the IgG (Fig. 4D), although the IgG aggregates were smaller and more widely distributed throughout the cytoplasm than the IgM aggregates.

Cell Surface Expression of VH56R+V κ 38c. Given the intracellular accumulation of VH56R+V κ 38c, we wondered whether this Ab reaches the cell surface. Indeed, the VH56R+V κ 38c and VH56R/76R+V κ 38c IgM, rather than being degraded, appeared in clusters at the plasma membrane (Fig. 4A and C, arrowheads). To test whether this IgM is also exposed at the cell surface, we stained live hybridomas (see *Methods*) and observed that the VH56R+V κ 38c IgM forms large surface IgM clusters (Fig. 4I). Such large surface IgM clusters were not observed on >200 cells expressing VH56R+V κ 21D. Moreover, the surface density of VH56R+V κ 38c IgM was higher than VH56R+V κ 21D. Thus, even though VH56R+V κ 38c and VH56R/76R+V κ 38c IgM accumulate in the cytoplasm, analysis of hybridomas suggested that these antibodies also translocate to the cell surface.

Even though VH56R+V κ 38c hybridomas accumulate intracellular IgM and express IgM at the cell surface, the distribution of IgM *in vivo* might be different. If Golgi binding blocks or delays antibody transport to the cell surface, then surface levels of VH56R+V κ 38c IgM may be reduced compared with other VH/V κ pairs. To determine surface IgM levels in newly forming B cells, we analyzed B220⁺, AA4.1⁺ cells (Hardy fraction E) in the bone marrow of VH56R Tg C57BL/6 mice. We used κ staining to compare surface IgM levels in B cells expressing the IgM^a allotype (which should include VH56R+V κ 38c-expressing B cells) to B cells expressing the IgM^b allotype. In two independent experiments (one of which is shown in SI Fig. 7), we observed reduced κ surface staining in IgM^a compared with IgM^b cells. A lower level of κ expression was also observed in

IgM^{a+} recirculating bone marrow B cells (Hardy fraction F), splenic transitional cells, and mature B cells from VH56R Tg C57BL/6 mice (SI Fig. 7). These findings are consistent with the model that binding to an intracellular antigen impairs antibody trafficking to the cell surface.

To examine the intracellular distribution of IgM in primary B lymphocytes, we isolated B cells from the spleen of a VH56R Tg mouse and maintained them in short-term culture before confocal microscopy. We sorted for IgM^a-positive B cells to exclude cells expressing endogenous VH from our analysis (Fig. 4K). Approximately one-third (35%) of B cells exhibited intracellular IgM, the distribution and density of which were comparable to the intracellular IgM of VH56R+V κ 38c hybridomas. In addition, some of the IgM receptors formed clusters at the cell surface (Fig. 4K).

VH56R+V κ 38c Receptors Are Enriched in Marginal Zone (MZ) B Cells.

To analyze the expression of VH56R+V κ 38c BCR in B cell subsets, splenocytes were sorted as transitional (B220⁺, AA4.1⁺), follicular (Fo; IgM^a^{int}, CD21^{int}), and MZ (IgM^a^{hi}, CD21^{hi}) B cells (Fig. 5A and B). Rearrangements of V κ 38c to J κ 4 and J κ 5, the main products of editing by V κ 38c, were measured in each of the subsets by quantitative PCR of genomic DNA. The results are depicted as fold differences relative to IgM⁺ κ ⁺ cells from wild-type C57BL/6 mice (Fig. 5C). In transitional cells, there was a 2-fold increase over wild-type mice in the use of V κ 38c. However, compared with wild-type B cells, V κ 38c was enriched \approx 6-fold in Fo B cells and nearly 12-fold in MZ B cells. These results suggested that VH56R+V κ 38c B cells preferentially acquire a MZ phenotype and accumulate in the splenic MZ. Because the MZ is expanded in VH56R mice, in absolute numbers, there are nearly twice as many MZ than Fo B cells that express VH56R+V κ 38c.

Using surface IgM density as a basis for assigning B cells to the MZ subset could be problematic in the case of IgMs with unusual distribution or trafficking in B cells. To provide an independent measure of VH56R+V κ 38c use in the major B cell subsets, and to examine VH56R and V κ 38c use in individual cells, we separated B cells based on CD21 and CD23 expression (Fig. 5D–G) and analyzed their VH and VL use by single-cell V gene RT-PCR. We observed that 35% of MZ B cells expressed both VH56R and V κ 38c (Fig. 5H) compared with only 17% of Fo B cells (Fig. 5I). This result confirmed the data from the quantitative PCR analyses and established that the MZ contains the highest accumulation of the autoreactive VH56R+V κ 38c pair in the spleen. Moreover, these results indicated that V κ 38c and VH56R are coexpressed in individual MZ B cells, a result that could not be derived from quantitative PCR with B cell populations.

Discussion

B cells become tolerant to self-antigens by replacing autoreactive L chains with L chains that suppress or modify the original autoreactivity. Several L chains edit anti-dsDNA reactivity; e.g., V κ 21D, combined with the anti-dsDNA VH56R, modifies the combining site (22) so as to curtail dsDNA binding (Fig. 2A). Other L chains such as V κ 8 decrease affinity for dsDNA, and VH3H9+V κ 8 B cells are in the periphery in a quasi-anegetic state (8). Also in the periphery is the combination of VH56R+V κ 38c, even though V κ 38c does not decrease dsDNA binding (Fig. 2C). Our data suggest a possible reason for the escape of this VH/VL pair from central tolerance: The VH56R/V κ 38c has an additional specificity for a Golgi-associated antigen (Fig. 3A). Because newly synthesized IgM must transit through the Golgi on its way to the cell surface, the binding of VH56R+V κ 38c IgM to the Golgi may delay surface IgM expression.

Consistent with this idea, surface κ staining is less intense in IgM^a than in IgM^b B cells (SI Fig. 7). Clearly, alternative explanations for the reduced levels of surface Ig in IgM^a B cells

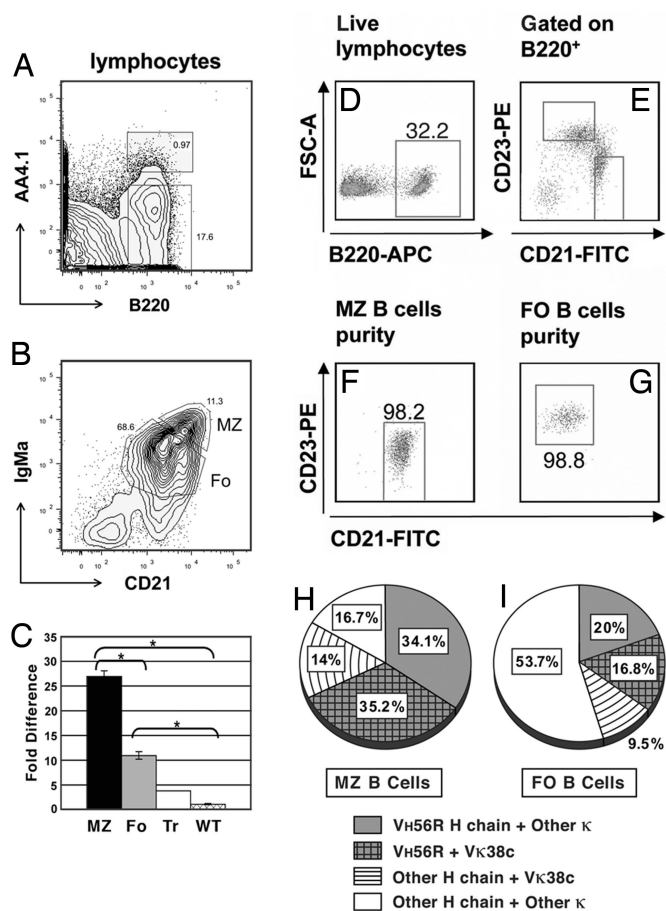


Fig. 5. V κ 38c-J κ 5 L chain rearrangements in peripheral B lymphocyte subsets. Lymphocytes from the spleen of a VH56R/B6 mouse were separated into transitional and mature B cell fractions based on B220 and AA4.1 expression (A). B220⁺ splenocytes were further separated into MZ and Fo B cell subsets (B). Quantitative PCR was used to determine V κ 38c-J κ 5 L chain rearrangements in IgM^a peripheral subsets (C). V κ 38c-J κ 5 rearrangements are depicted relative to a C57BL/6 wild-type mouse. Significance levels were determined by two-tailed Student's *t* test: *, *P* ≤ 0.01. Alternatively, B220⁺ lymphocytes (D) were sorted into MZ (CD21^{hi} CD23^{int}) and Fo B cells (CD21^{int} CD23^{hi}), as previously reported (15) (E). Purity of sorted MZ and Fo B cells was 98.2% and 98.8%, respectively (F and G). Single-cell RT-PCR identified VH56R and V κ 38c rearrangements. The MZ (H) has almost twice the number of VH56R+V κ 38c cells (35.2%) compared with the Fo (16.8%; I). Approximately 34% of the cells in the MZ have VH56R and a L chain other than V κ 38c, whereas V κ 38c is associated with an endogenous H chain in 14% of the cells (H). In 9.5% of the Fo B cells, V κ 38c is associated with an endogenous H chain (I).

may apply, e.g., L chain editing and/or surface Ig down-regulation (7, 11, 26, 27).

It is well established that intracellular Ig signals can promote B cell development. In pre-B cells, the pre-B receptor acts from an intracellular location to generate most, if not all, signals that promote B cell differentiation (31). Similarly, intracellular IgM may be competent for signaling because the BCR assembles and associates with Ig α and Ig β in a post-endoplasmic reticulum (ER) compartment (32). Furthermore, there is precedent for the development of peripheral B cells whose BCR binds to an intracellular antigen: B cells that express IgM to hen egg lysozyme (HEL), together with an ER-anchored form of the antigen, block surface IgM expression by Ig retention in the ER, yet they develop into splenic Fo B cells (33).

Unlike the anti-HEL-ER B cells, the VH56R+V κ 38c B cells accumulate IgM in the Golgi but nevertheless achieve high

surface IgM density (see *SI Text* and *SI Fig. 8*). In addition, they also acquire a MZ B cell phenotype (Fig. 5). The different outcomes in the anti-HEL-ER model and the anti-dsDNA-Golgi model may reflect differences in the sites of IgM accumulation. IgMs such as the anti-HEL-ER that accumulate in the ER may be diverted to aggresomes, sites of increased protein degradation (34), whereas the VH56R+V κ 38c IgM that accumulates in the Golgi may not be degraded. Consequently, accumulation of VH56R+V κ 38c IgM might induce the unfolded protein response, an adaptation known to play a role in the B cell response to antigen (35). The unfolded protein response may drive the VH56R+V κ 38c B cells to become surface IgM-bright because it increases the efficiency of IgM synthesis. The increased IgM synthesis may reach a level that exceeds the intracellular retention capacity of the Golgi. As a result, large IgM clusters may be transferred to the cell surface (Fig. 4I).

The surface expression of the autoreactive VH56R+V κ 38c IgM may be responsible for the increased abundance of VH56R+V κ 38c B cells in the MZ (Fig. 5). It has been argued that sustained signaling through the BCR promotes B cell homing to the splenic MZ (36). B cells sequestered in the MZ may play an important role in peripheral tolerance (37). Because MZ B cells usually lack help to undergo affinity maturation or switch isotype, they may be blocked in the secretion of pathogenic antibodies. This possibility could account for the fact that B cells expressing VH56R+V κ 38c receptors, despite being autoreactive and achieving high surface Ig density, do not spontaneously induce autoimmunity.

Methods

Binding Assays. The oligonucleotide primers, templates, and plasmids used in the construction of scFv expression vectors are described in *SI Text*, as are the methods for the expression and purification of bivalent scFv proteins. The recombinant Ab fragments were used in an antigen capture assay (18), whereas PS binding was assessed by direct immunoassay (17).

Cell Culture. Jurkat T cells (clone E6-1; American Type Culture Collection) were used to assess scFv binding (38, 39). B cell hybrids expressing VH56R+V κ 38c IgM (hybridoma 160.3) and VH56R+V κ 21D IgM (hybridoma 79.1) were derived from a VH56R mouse with graft-versus-host disease (15). In addition, we used VH56R/76R+V κ 38c IgM and IgG hybridomas (30) and a VH56R+V λ x IgM hybridoma (25). The hybridomas used in this study were analyzed by RT-PCR and ELISA to minimize the possibility of allelic and isotypic inclusion (15, 25).

Immunofluorescence and Confocal Microscopy. Cells were fixed with 6% paraformaldehyde for 15 min on ice and permeabilized with 0.075% Triton X-100. To identify the Golgi, Alexa Fluor 488-labeled lectin II (Invitrogen) was used. The IgM was visualized with Alexa Fluor 647-labeled goat anti-mouse IgM (Invitrogen), and DNA was stained with Sytox Orange (Invitrogen). Surface IgM was visualized by staining live cells on ice and in the presence of sodium azide. Bound scFv were detected with Alexa Fluor 647-conjugated rabbit anti-mouse IgG (Invitrogen). Samples were viewed on a Zeiss LSM510 laser scanning microscope, as described (38).

Animals. The VH56R Tg has been described previously (22, 29). VH56R mice were backcrossed on the C57BL/6 background for 10 generations.

Flow Cytometry. Splenocytes were harvested from VH56R mice and littermate controls, washed, and resuspended at 1×10^7 cells per milliliter for staining with the following Abs: FITC CD21 (clone 7G6), phycoerythrin CD23 (clone B3B4), and biotin IgMa (clone DS-1) (all from BD Pharmingen), as well as allophycocyanin AA4.1 and B220 allophycocyanin-Cy7 (from eBiosciences), and our own anti-IgM^a antibody, RS 3.1, conjugated to Alexa Fluor 488. Stained samples were analyzed and sorted on a FACSVantage SE Cell Sorter (BD Biosciences). Flow cytometric data were analyzed by using FlowJo version 6.4.7 software (TreeStar). To examine intracellular IgM in B cells, splenocytes from one VH56R mouse were sorted for IgM^a-low surface phenotype and cultured in RPMI medium 1640 with 10% FCS, 10 μ M 2-mercaptoethanol, and antibiotics for 48 h. At the end of that period, cells were harvested and prepared for confocal microscopy, as described above.

Quantitative PCR. Genomic DNA was purified from sorted cells and used for quantitative PCR (40°C for 10 min, 95°C for 10 min, followed by 60 cycles at 95°C for 10 sec, 60°C for 30 sec, and 72°C for 1 sec), as suggested for the LightCycler 480 real-time PCR system (Roche Applied Science). The V κ 38c-J κ 5 product was amplified with forward primer (5'-CTC ATA CAT TAC ACA TCT ACA TTA CAG CC-3') and reverse primer (5'-TGC CAC GTC AAC TGA TAA TGA GCC CTC TC-3') and detected with a FAM-labeled hydrolysis probe (5-TCC TTC AGC ATC AGC AAC CTG-3'). For each sample, the V κ 38c-J κ 5 product was normalized to a β -actin PCR product and compared with wild-type C57BL/6 B220⁺ IgM⁺ κ ⁺ splenocytes.

Single-Cell Sorting, cDNA Synthesis, and PCR. IgM^a-bright (CD19⁺ IgM allotype b-IgM allotype a^{high}), IgM^a-dim (CD19⁺ IgM allotype b-IgM allotype a^{low}), MZ (B220⁺ CD21^{hi} CD23^{int}), and Fo B cells (B220⁺ CD21^{int} CD23^{hi}) from one VH56R/B6 mouse were sorted, and Ig gene rearrangements were assayed by using primers for VH56R, V κ 38c, and a degenerate V κ (s) primer with nested C κ reverse primers, as previously described (15). We sequenced 76 V κ 38c-

positive PCR products from individual wells in five 96-well plates. Of these, 75 sequences matched V κ 38c in-frame rearrangements.

Additional Details. Our SI includes the procedures used to construct, express, and purify the recombinant scFv, as well as the gel electrophoretic analysis of the purified scFv (SI Fig. 6). The surface density of BCR on IgM^a- and IgM^b-expressing B cells was assessed by flow cytometry at different stages of B cell development (SI Fig. 7). In addition, we present data on the VH and V κ use in IgM^a-bright and IgM^a-dim splenocytes from VH56R knockin C57BL/6 mice (SI Fig. 8).

ACKNOWLEDGMENTS. We thank Drs. Tony Marion and Kerstin Kiefer for critical comments and Mr. Tim Higgins for expert assistance with graphical arts. This work was funded by grants from the Lupus Research Institute, the University of Tennessee Center of Excellence for Diseases of Connective Tissue, and the National Institutes of Health. S.N.K. acknowledges the Robert and Richard Rizzo Award from the University of Tennessee Health Sciences Center.

- Radic MZ, Zouali M (1996) Receptor editing, immune diversification, and self-tolerance. *Immunity* 5:505–511.
- Nemazee D (2000) Receptor selection in B and T lymphocytes. *Annu Rev Immunol* 18:19–51.
- Tiegs SL, Russell DM, Nemazee D (1993) Receptor editing in self-reactive bone marrow B cells. *J Exp Med* 177:1009–1020.
- Radic MZ, Erikson J, Litwin S, Weigert M (1993) B lymphocytes may escape tolerance by revising their antigen receptors. *J Exp Med* 177:1165–1173.
- Prak EL, Weigert M (1995) Light chain replacement: A new model for antibody gene rearrangement. *J Exp Med* 182:541–548.
- Chen C, Nagy Z, Prak EL, Weigert M (1995) Immunoglobulin heavy chain gene replacement: A mechanism of receptor editing. *Immunity* 3:747–755.
- Chen C, et al. (1995) The site and stage of anti-DNA B-cell deletion. *Nature* 373:252–255.
- Xu H, Li H, Suri-Payer E, Hardy RR, Weigert M (1998) Regulation of anti-DNA B cells in recombination-activating gene-deficient mice. *J Exp Med* 188:1247–1254.
- Wardemann H, et al. (2003) Predominant autoantibody production by early human B cell precursors. *Science* 301:1374–1377.
- Retter MW, Nemazee D (1998) Receptor editing occurs frequently during normal B cell development. *J Exp Med* 188:1231–1238.
- Casellas R, et al. (2007) Ig κ allelic inclusion is a consequence of receptor editing. *J Exp Med* 204:153–160.
- Brard F, Shannon M, Prak EL, Litwin S, Weigert M (1999) Somatic mutation and light chain rearrangement generate autoimmunity in anti-single-stranded DNA transgenic MRL/lpr mice. *J Exp Med* 190:691–704.
- Sekiguchi DR, Eisenberg RA, Weigert M (2003) Secondary heavy chain rearrangement: A mechanism for generating anti-double-stranded DNA B cells. *J Exp Med* 197:27–39.
- Sekiguchi DR, et al. (2006) Development and selection of edited B cells in B6.56R mice. *J Immunol* 176:6879–6887.
- Witsch EJ, Cao H, Fukuyama H, Weigert M (2006) Light chain editing generates polyreactive antibodies in chronic graft-versus-host reaction. *J Exp Med* 203:1761–1772.
- Shlomchik MJ, Aucoin AH, Pisetsky DS, Weigert MG (1987) Structure and function of anti-DNA autoantibodies derived from a single autoimmune mouse. *Proc Natl Acad Sci USA* 84:9150–9154.
- Cocca BA, et al. (2001) Structural basis for autoantibody recognition of phosphatidylserine- β 2 glycoprotein I and apoptotic cells. *Proc Natl Acad Sci USA* 98:13826–13831.
- Radic MZ, et al. (1993) Residues that mediate DNA binding of autoimmune antibodies. *J Immunol* 150:4966–4977.
- Seal SN, Monestier M, Radic MZ (2000) Diverse roles for the third complementarity determining region of the heavy chain (H3) in the binding of immunoglobulin Fv fragments to DNA, nucleosomes and cardiolipin. *Eur J Immunol* 30:3432–3440.
- Radic MZ, Mascelli MA, Erikson J, Shan H, Weigert M (1991) Ig H and L chain contributions to autoimmune specificities. *J Immunol* 146:176–182.
- Neeli I, et al. (2007) Divergent members of a single autoreactive B cell clone retain specificity for apoptotic blebs. *Mol Immunol* 44:1924–1931.
- Li H, Jiang Y, Prak EL, Radic M, Weigert M (2001) Editors and editing of anti-DNA receptors. *Immunity* 15:947–957.
- Li Y, Li H, Weigert M (2002) Autoreactive B cells in the marginal zone that express dual receptors. *J Exp Med* 195:181–188.
- Li Y, Louzoun Y, Weigert M (2004) Editing anti-DNA B cells by V λ x. *J Exp Med* 199:337–346.
- Doyle CM, Han J, Weigert MG, Prak ET (2006) Consequences of receptor editing at the λ locus: Multireactivity and light chain secretion. *Proc Natl Acad Sci USA* 103:11264–11269.
- Liu S, et al. (2005) Receptor editing can lead to allelic inclusion and development of B cells that retain antibodies reacting with high avidity autoantigens. *J Immunol* 175:5067–5076.
- Huang H, Kearney JF, Grusby MJ, Benoist C, Mathis D (2006) Induction of tolerance in arthritogenic B cells with receptors of differing affinity for self-antigen. *Proc Natl Acad Sci USA* 103:3734–3739.
- Gerdes T, Wabl M (2004) Autoreactivity and allelic inclusion in a B cell nuclear transfer mouse. *Nat Immunol* 5:1282–1287.
- Radic MZ, Weigert M (1994) Genetic and structural evidence for antigen selection of anti-DNA antibodies. *Annu Rev Immunol* 12:487–520.
- Chen C, et al. (2006) Selection of anti-double-stranded DNA B cells in autoimmune MRL-lpr/lpr mice. *J Immunol* 176:5183–5190.
- Guloglu FB, Roman CA (2006) Precursor B cell receptor signaling activity can be uncoupled from surface expression. *J Immunol* 176:6862–6872.
- Mielenz D, Ruschel A, Vettermann C, Jack HM (2003) Immunoglobulin μ heavy chains do not mediate tyrosine phosphorylation of Ig α from the ER-cis-Golgi. *J Immunol* 171:3091–3101.
- Ferry H, Jones M, Vaux DJ, Roberts IS, Cornall RJ (2003) The cellular location of self-antigen determines the positive and negative selection of autoreactive B cells. *J Exp Med* 198:1415–1425.
- Kopito RR, Sittia R (2000) Aggresomes and Russell bodies. Symptoms of cellular indigestion? *EMBO Rep* 1:225–231.
- Skalet AH, et al. (2005) Rapid B cell receptor-induced unfolded protein response in nonsecretory B cells correlates with pro- versus antiapoptotic cell fate. *J Biol Chem* 280:39762–39771.
- Martin F, Kearney JF (2002) Marginal-zone B cells. *Nat Rev Immunol* 2:323–335.
- Lopes-Carvalho T, Foote J, Kearney JF (2005) Marginal zone B cells in lymphocyte activation and regulation. *Curr Opin Immunol* 17:244–250.
- Radic M, Marion T, Monestier M (2004) Nucleosomes are exposed at the cell surface in apoptosis. *J Immunol* 172:6692–6700.
- Cocca BA, Cline AM, Radic MZ (2002) Blebs and apoptotic bodies are B cell autoantigens. *J Immunol* 169:159–166.